# Measured and Simulated Strain in the Large Scale Coil With Considering Winding Compressibility

Shannon R. Griffin, Yu Suetomi, Ernesto Bosque, Kwangmin Kim, Jun Lu, Hongyu Bai, and Iain Dixon, *Senior Member, IEEE*

***Abstract*—The Large Scale Coil (LSC) is a high-temperature superconducting (HTS) coil that has been developed and tested in the research and development efforts for the 40-T All-Superconducting Magnet Project at the National High Magnetic Field Laboratory (NHMFL). The LSC is composed of stacked pancake disks consisting of 2-in-hand wound rare-earth barium copper oxide coated conductor (CC REBCO) tapes with stainless steel and copper co-wind. Under high magnetic fields, Lorentz forces on the REBCO tapes can impact the performance of the coil. Experimental strain data was collected and compared to simulated results. Initial results reveal significantly higher simulated strain at both inboard and outboard gauges. Manufactured REBCO have thickness variations along tape width. Similarly, stainless steel tapes used for over-banding have microscopic surface asperities. These tapes were initially assumed to be perfectly flat and had a "hard contact" condition in simulations. Comparison of experimental results to simulations reveal that incorporating these aspects of REBCO tape surface structure decreases the difference between simulated and experimental results for particular cases. In addition, edge friction effects due to "axial clamping" were simulated, and resulting strain was compared to experimental data. Strain data from the LSC tests are a valuable resource for verification of modeling methods and improving our understanding and design of large and complex HTS magnets such as the 40-T. This investigation compares measured strain data with simulated strain to assess and improve our current modeling techniques for HTS coil design.**

***Index Terms*—High field magnet, high-temperature superconductors, REBCO coil, screening current induced stress, strain analysis.**

## I. Introduction

THE 40T all-superconducting magnet is currently in development at the National High Magnetic Field Laboratory (NHMFL). As a user magnet, the 40T will contribute to advanced research in physics, biology, and chemistry. It will be designed to achieve a 40 T field with low noise and a cold bore of 34 mm. Other design objectives are detailed in [1].

The Large Scale Coil (LSC) was developed and built in efforts for the 40T-all superconducting magnet project. Like the 40T, disks in the LSC are comprised of 2-in-hand rare-earth barium copper oxide coated conductor (CC REBCO) wound with stainless steel and copper co-wind, with a stainless-steel over-banding.

REBCO is a popular superconductor choice in high-field magnet construction due to high critical current density, high critical magnetic field, and high critical temperature, along with its commercial availability due to its use in fusion magnet development [2]. In HTS coils, REBCO tapes may undergo irreversible damage due to high strains [3], [4]. Strains which may not cause immediate damage to the coil may affect performance over time due to fatigue [5]. As a user magnet, the 40T will undergo many ramping and de-ramping cycles [1]. Therefore, when designing HTS coils for high fields, it is important to consider strain in the winding pack.

Recently, it was experimentally proven that stacks of REBCO tapes have a lower Young's modulus in the stacked direction compared to that of one REBCO tape, and a non-linear stress-strain curve [6], due to microscopic asperities on the tape surface and tape thickness profiles [7]. This has also been experimentally confirmed in pancake coils and is referred to as winding compressibility [7], [8].

Disks closer to the midplane experience axial clamping due to axial forces [9]. As a result, friction between the edge of the tapes and the spacers may affect tape motion and tilt.

A series of experiments were conducted in 2024–2025. Data collected from inboard and outboard strain gauges during LSC experiments were compared to simulations. Simulated strain at inboard and outboard locations on the disk were consistently higher than measured data, prompting an investigation. Two aspects that were investigated computationally were how macroscopic and microscopic roughness affect the radial compressibility of HTS disks, and how edge friction effects strain in HTS disks, particularly in disks near the midplane.

## II. Experimental Methods

The LSC consists of 22 double-pancake modules and is mirrored about the midplane. LSC insert parameters are in Table I. A schematic of the LSC insert with labeled disk numbers are shown in Fig. 1. a. Stainless steel over-banding was wound on

Received 28 July 2025; revised 3 October 2025 and 28 October 2025; accepted 29 October 2025. Date of publication 10 November 2025; date of current version 25 November 2025. This work was supported by the National Science Foundation Cooperative which was performed at the National High Magnetic Field Laboratory under Agreement DMR-2131790 and Agreement DMR-2128556 and in part by the State of Florida. *(Corresponding author: Shannon R. Griffin.)*

Shannon R. Griffin, Yu Suetomi, Kwangmin Kim, Jun Lu, Hongyu Bai, and Iain Dixon are with the National High Magnetic Field Laboratory, Florida State University, Tallahassee, FL 32320 USA (e-mail: sgriffin@magnet.fsu.edu).

Ernesto Bosque is with the National High Magnetic Field Laboratory, Tallahassee, FL 32320 USA. He is now with the Magnetics Corporation Tallahassee, FL 32301 USA.

Color versions of one or more figures in this article are available at https://doi.org/10.1109/TASC.2025.3630115.

Digital Object Identifier 10.1109/TASC.2025.3630115

TABLE I
LSC INSERT PARAMETERS

| Inner Radius [mm] | Outer Radius [mm] | Coil half Height [mm] | Turns per pancake | REBCO thickness [μm] | Steel co-wind thickness [μm] | Copper co-wind thickness [μm] |
|---|---|---|---|---|---|---|
| 130 | 161 | 96.8 | 35-56 | 95*2/4.1 | 150 | 127 |

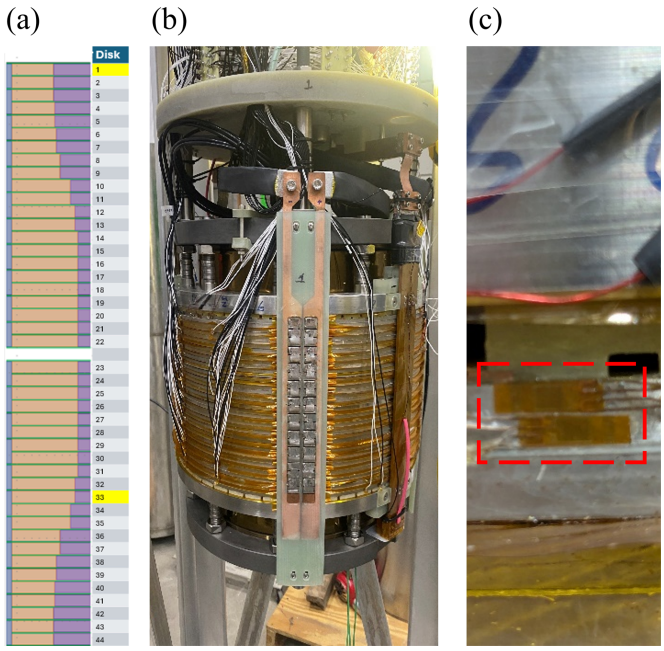


Fig. 1. (a) Schematic of disks in the LSC. Strain data from disks highlighted yellow was used in this study. The winding pack is indicated in beige, and the over-banding is purple. (b) A picture of the LSC insert. (c) A picture of strain gauges on disk 1 of the LSC. Strain gauges indicated by the red dashed rectangle. For this disk, the inboard gauge (closer to the midplane), is the bottom gauge, and the outboard gauge (further from the midplane), is the top gauge.

the outside of the disks. Co-winds and over-banding were added to the design for structural support. The number of turns in the winding and number of layers of over-banding are dependent on each disk. Disks further away from the midplane experience more screening currents and therefore have more over-banding for structural support. This can be seen in Fig. 1(a).

The LSC was operated in an 11.4 T background field, provided by the 45T magnet outsert [10]. The LSC was designed to ramp to 645 A and produce a combined field of 16.5 T at the magnet center.

A series of tests were performed in 2024–2025. Strain was measured with type WK-06-230DS-350 gauges connected to a D4 DAC module, both from MicroMeasurements. Strain gauges were placed on the inboard and outboard edges of the outer turn of the over-banding. Inboard and outboard are in reference to the edge of the disk that is furthest from the midplane (outboard) and closest to the midplane (inboard). A picture of the strain gauges on disk 1 is shown in Fig. 1(c). Compensation gauges were also attached to account for the magnetic field. All data that is shown in this study is compensated for the magnetic field with data from the compensation gauges.

TABLE II
STRUCTURAL SIMULATION PARAMETERS

| Material | Parameters |
|---|---|
| REBCO | $E_\theta$ = 143.0 [GPa], $E_r$ = 104.7 [GPa], $E_z$ = 142.1[GPa] $\nu_{r\theta}$ = 0.321, $\nu_{\theta z}$ = 0.322, $\nu_{rz}$ = 0.321 |
| Stainless steel co-wind | E = 186 [GPa] ν = 0.282 |
| Copper co-wind | E = 22.9 [GPa] ν = 0.34 |
| Stainless steel over-banding | E = 186 [GPa] ν = 0.282 |

Strain data from these runs was collected and compared amongst each other for repeatability. Data from disk 33 and disk 1 from dual operation to 614 A, were used for comparisons to simulations in this study. During dual operation to 614 A, the outsert is first charged to 11.4 T. Gauges are zeroed out at the beginning of the outsert charge. Measured strain during outsert charge was observed to be negligible. After the outsert charge, the LSC insert is then charged to 614 A.

## III. SIMULATION METHODS

As a baseline numerical simulation model, Florida Screening Strain Software (FLOSSS) was used [11], [12], [13]. FLOSSS employs a T-A formulation [14] to calculate current density and magnetic field, coupled with a structural mechanics model for one module (two disks) at once. At each timestep, the structural mechanics model applies the Lorentz force, calculated from the electromagnetics model, as a body load on the REBCO tapes. Young's modulus and Poisson's ratio of winding pack and over-banding materials are tabulated in Table II. The resulting tape tilt is then applied in the electromagnetics model for that module, at the next timestep. Winding stress and thermal contraction are also considered. Critical current is calculated using a sin-squared-fit function. Based on this simulation model, the following characteristics were additionally considered.

### A. Winding Compressibility for REBCO Tapes

In the base model, the mechanical properties of the REBCO tapes were computed using the rule of mixtures [15]. Therefore, the radial elastic modulus of the HTS disk was determined solely by the properties of each layer of material, assuming tapes to be perfectly flat, with a "hard contact" condition enforced at contact boundaries. As mentioned in the introduction, winding compressibility is caused by microscopic asperities on the tape surface, and the tape thickness profile. To incorporate the tape surface profile into our simulation model, we have developed a modeling technique called a Penalty Function with Gap Offset (PGO) that is detailed in a separate study [16]. In this approach, the tape profile is incorporated as a gap offset distributed across the tape width within the standard penalty method. The profile varies with each spool, and the measured profiles of REBCO used in disk 1 and disk 33 are displayed in Fig. 2.

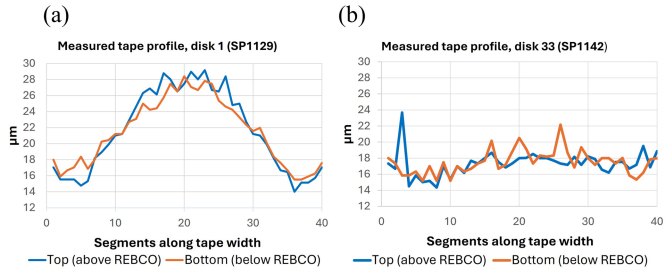


Fig. 2. Measured tape profile in micrometers across the width of the REBCO tape. (a) Tape used in disk 1. (b) Tape used in disk 2.

### B. Winding Compressibility for the Over-Banding

Further, in the base model, the stainless-steel tapes comprising the over-banding were also assumed to be without winding compressibility. This is inaccurate, due to microscopic asperities on their surface, resulting in the actual radial elastic modulus of the stainless-steel over-banding to be lower than the elastic modulus of stainless steel [7]. In [7], a compressibility model was detailed and fit to experimentally determined data. This model was implemented into FLOSSS for the stainless-steel over-banding as a penalty factor, via the contact physics between turns. For a pancake composed of stainless-steel tapes, pressure can be written as a function of the allowed penalty between turns, $g_n$.

$$p\ (g_n) = -\log_e\left(\frac{g_n}{l_0}+1\right)/\lambda \tag{1}$$

Where $l_0$ is the initial distance between turns, and $\lambda$ is a constant [7].

### C. Edge Friction Due to Axial Clamping

Axial clamping due to accumulated forces from pancakes above and below pressing on disks causes friction between the spacers and tape edges, opposing tape tilt as tapes move during insert charging. Edge friction was modeled in FLOSSS using the simplified friction equation for convergence

$$F_{ed} = -\mu_{ed} F_z. \tag{2}$$

Where $F_{ed}$ is edge friction, $\mu_{ed}$ is the frictional coefficient (assumed as 0.2), and $F_z$ is axial force. Axial pressure on each disk was computed in a simplified LSC model, which models each disk as a homogenized region, and imported. Friction force and axial force were applied as boundary conditions.

## IV. Results and Discussion

Initial comparisons using the base simulation model reveal that predicted strain on the inboard and outboard edges of the disks are consistently higher than what is measured (see Fig. 3). The difference between inboard and outboard strain for a disk indicates how much tilt is on the outside turn of the over-banding. This tilt on the outside of the over-banding is predicted to be larger than what was experimentally measured for disk 33. The effect of simulating a low elastic radial modulus due to macroscopic roughness in the winding pack, microscopic roughness in the over-banding, and edge friction is subsequently investigated. Implementation of these effects involved applying Lorentz forces from the base FLOSSS model at the time of interest in a stationary study, rather than a fully-coupled electromagnetic-structural simulation, which presents significant computational challenges. We note that this may not fully capture stress relaxation, however, the present study focused on analyzing the effects of winding compressibility and edge friction.

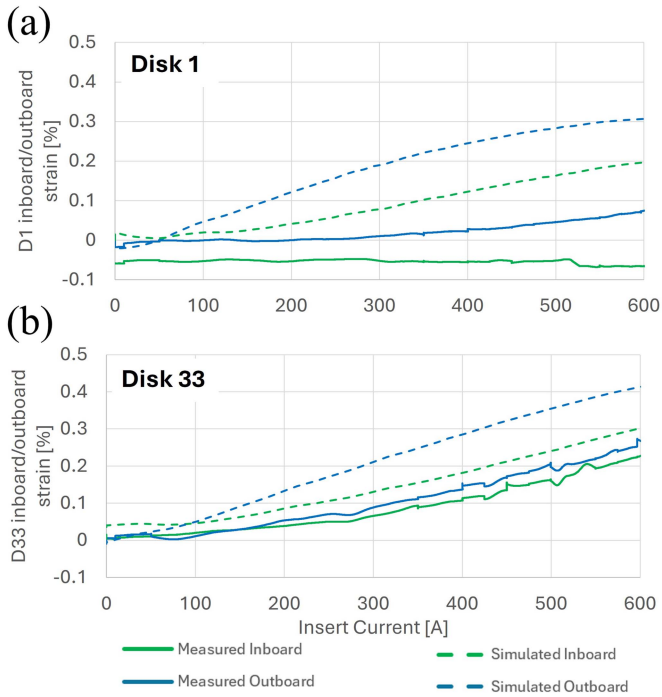


Fig. 3. (a) measured and (b) simulated strain. Simulated strain is evaluated at locations on the disk akin to the placement of inboard and outboard strain gauges in experiments. Simulations assume tapes to be flat.

### A. Effects of Winding Compressibility

Predicted strain while considering winding compressibility due to the REBCO tape profile, and microscopic asperities on the stainless-steel over-banding, is displayed as plots in Fig. 4, also showing predicted strain from base simulation model (dashed line), and measured strain (solid line).

Accounting for the winding compressibility of the REBCO tapes and the over-banding lowers the effective radial modulus of the pancakes. Therefore, the strain that occurs in the REBCO does not transfer to the outside of the over-banding as effectively. The strain values where the strain gauges are located are less than originally predicted, and closer to the measured data for disk 1. The difference between minimum and maximum thickness in the REBCO tape profile for disk 1 is relatively large, compared to the tape used in disk 33. Disk 1 also has a thick over-banding section compared to disk 33. Therefore, the application of both a gap offset in the winding pack and compressibility model on the over-banding has a much greater impact on the predicted strain in disk 1.

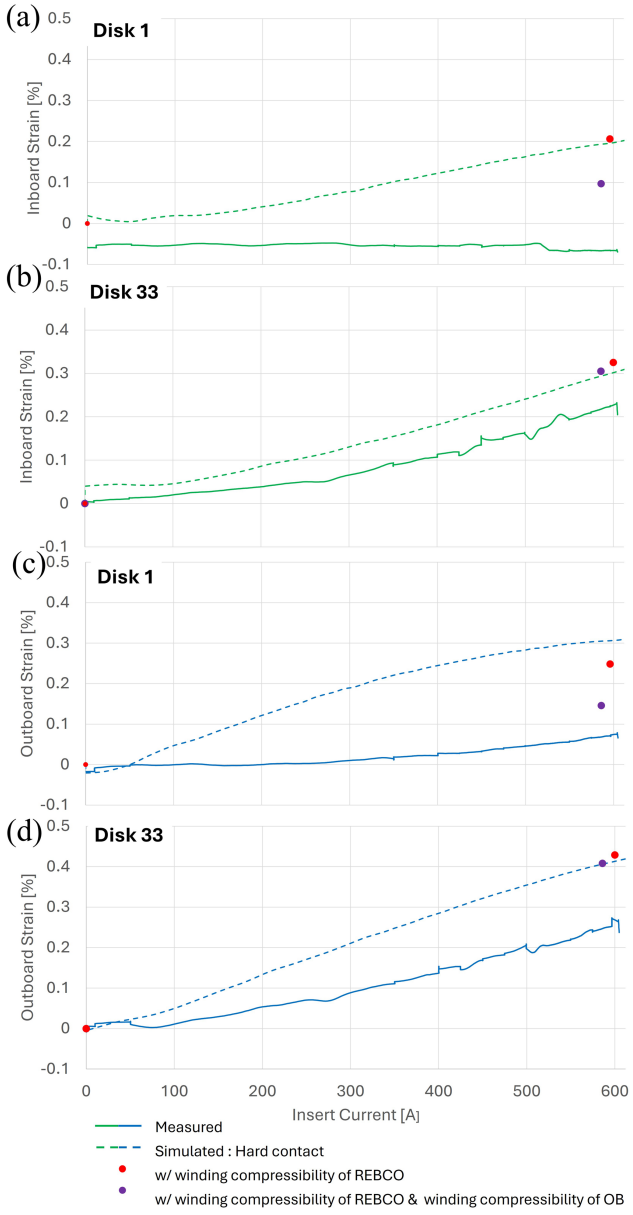


Fig. 4. Measured and simulated strain comparing original simulation (hard contact) results with results accounting for winding compressibility for the REBCO tapes and the stainless-steel over-banding.

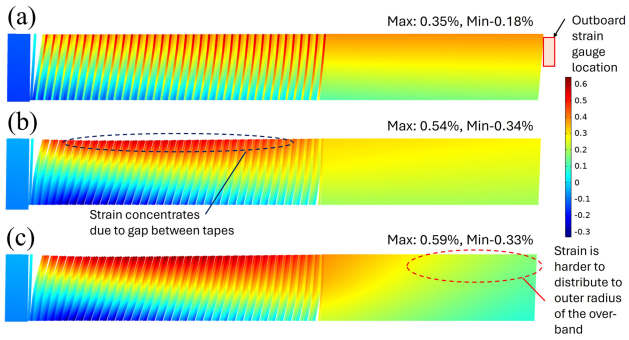


Fig. 5. Simulated hoop strain distribution [%], for disk 1 with a (a) hard contact condition, (b) winding compressibility on the REBCO tapes, and (c) both winding compressibility on the REBCO tapes and the over-banding.

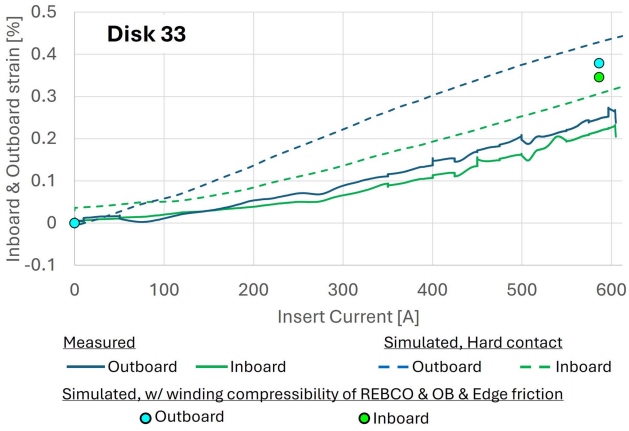


Fig. 6. Measured and predicted strain on inboard and outboard strain gauge locations on disk 33. Predicted strain accounts for edge friction.

Although this phenomenon accounts for less strain at the end of the over-banding, it does not mean that there is less strain in the winding pack. Conversely, this indicates that there is higher strain in the winding pack than originally predicted. Where tapes are thicker, the pancake is more rigid. Where the tape profile is thinner, the pancake is more radially elastic. This is because these thin regions at the edges of the tapes cause gaps in the winding pack. This can be seen in Fig. 5, when gap offset method is applied, strain concentrates in the winding pack due to these gaps. In addition, due to the radial compressibility of the over-banding, the pancake is not as well supported by the over-banding as originally predicted. In magnets that are designed for long-term operation, this strain must be mitigated, to avoid fatigue damage. Due to these findings, we are implementing thicker co-winds in our Large Scale Coil 2 and have updated the 40T design with thicker co-winds to account for high strain in the winding pack due to radial compressibility.

Increase in predicted strain in the winding pack is dependent on the tape profile of the REBCO tapes, as disks made with tapes that have a large 'hump' in the center, like the tape used in disk 1, are predicted to have higher strain in the winding pack. In comparison, disks that are manufactured with REBCO tapes with a flat, or 'dogbone' tape profile, like the tape used in disk 33, do not result in an increase in predicted strain when tape profile is considered. This can be seen when comparing the results of disk 1 disk 33 (see Fig. 4.).

### B. *Edge Friction*

Disk 33 is located near the midplane, and therefore subject to axial clamping, Disk 1 is located at the coil end, and therefore is not subject to axial clamping. Therefore, friction forces resist tape tilt in disk 33 [9]. Results of disk 33 while modeling edge friction are displayed in Fig. 6.

Although magnitude of strain is still higher than measured results, accounting for edge friction results in a tilt angle at the end of the over-banding that is akin to measured results. This supports the argument that edge friction is a factor that reduces tape tilt in disks near the midplane.

Even with factoring in edge friction, measured inboard and outboard strain is still lower than measured results. This is also the case for the predicted results for disk 1, while considering radial compressibility. This could be due to microscopic roughness on the tapes in the winding pack, which were not considered in the simulations. This indicates that the radial elastic modulus is even lower than what was implemented in these simulations, and winding pack strain is even higher than predicted.

## V. Conclusion

Strain in high-field HTS magnets is difficult to accurately predict via simulations due to the uncertainty of many factors that go into modeling HTS pancakes, particularly the variability in REBCO tapes that are used to manufacture these magnets. Winding compressibility is a factor that must be considered when designing HTS pancake disks. Depending on the macroscopic tape profile of the REBCO tape used, strain in winding pack may be much higher than originally predicted. A lower measured strain on the outer turn of the over-banding may actually indicate that strain in the winding pack is higher than what is predicted, particularly if the prediction assumes tapes to be perfectly flat.

Future investigations will involve implementing data from measured stress/strain curves of tape stacks measured here at NHMFL, into FLOSSS simulations, to more accurately model the radial elastic modulus in HTS pancake disks.

## References

[1] H. Bai et al., "The 40 T superconducting magnet project at the national high magnetic field laboratory," *IEEE Trans. Appl. Supercond.*, vol. 30, no. 4, Jun. 2020, Art. no. 4300405.

[2] X. Wang et al., "REBCO – A silver bullet for our next high-field magnet and collider budget?," in *Proc. US Community Study Future Part. Phys. (Snowmass 2022)*, 2022.

[3] C. Zhou, K. A. Yagotintsev, P. Gao, T. J. Haugan, D. C. van der Laan, and A. Nijhuis, "Critical current of various REBCO tapes under uniaxial strain," *IEEE Trans. Appl. Supercond.*, vol. 26, no. 4, Jun. 2016, Art. no. 8401304.

[4] K. Ilin et al., "Experiments and FE modeling of stressstrain state in ReBCO tape under tensile, torsional and transverse load," *Supercond. Sci. Technol.*, vol. 28, 2015, Art. no. 055006.

[5] K. B. Ashok, R. J. Thomas, M. J. Prakash, and A. Nijhuis, "Influence of fatigue on superconducting REBCO tapes under repeated cyclic tensile, bending and twisting loads: A simulation-based investigation," *Cryogenics*, vol. 132, 2023, Art. no. 103672.

[6] S. Xue, J. Kwon, Y. Guo, T. Garg, M. D. Sumption, and E. W. Collings, "Compressive stress-strain behavior of REBCO coated conductors and cables," *IEEE Trans. Appl. Supercond.*, vol. 33, no. 5, Aug. 2023, Art. no. 4800706.

[7] Y. Yan et al., "Measurement and analysis of winding stresses in dry-wound pancake coils considering nonlinear compressive behaviors," *Supercond. Sci. Technol.*, vol. 36, Sep. 2023, Art. no. 115019.

[8] J. Park, J. Kim, Y. Yan, and S. Hahn, "Diameter change of dry wound REBCO solenoid pancake coil by winding tension," *IEEE Trans. Appl. Supercond.*, vol. 34, no. 5, Aug. 2024, Art. no. 8400605.

[9] D. Kolb-Bond, M. D. Bird, T. Painter, S. K. Ramakrishna, and A. Reyes, "Screening current induced field changes during de-energization with axial clamping," *IEEE Trans. Appl. Supercond.*, vol. 32, no. 6, Sep. 2022, Art. no. 4701404.

[10] J. R. Miller, "The NHMFL 45-T hybrid magnet system: Past, present, and future," *IEEE Trans. Appl. Supercond.*, vol. 13, no. 2, pp. 1385–1390, Jun. 2003.

[11] D. Kolb-Bond et al., "Screening current rotation effects: SCIF and strain in REBCO magnets," *Supercond. Sci. Technol.*, vol. 34, no. 9, 2021, Art. no. 095004.

[12] D. J. Kolb-Bond et al., "Computing strains due to screening currents in REBCO magnets," *IEEE Trans. Appl. Supercond.*, vol. 30, no. 4, Jun. 2020, Art. no. 4602805.

[13] Y. Suetomi et al., "Screening current induced stress/strain analysis of high field REBCO coils with co-winding or over-banding reinforcement," *IEEE Trans. Appl. Supercond.*, vol. 34, no. 5, Aug. 2024, Art. no. 8400206.

[14] F. Huber, W. Song, M. Zhang, and F. Grilli, "The T-A formulation: An efficient approach to model the macroscopic electromagnetic behaviour of HTS coated conductor applications," *Supercond. Sci. Technol.*, vol. 35, 2022, Art. no. 043003.

[15] W. D. Callister and D. G. Rethwisch, *Materials Science and Engineering: An Introduction*. Hoboken, NJ, USA: Wiley, 2014.

[16] Y. Suetomi et al., "Screening current-induced stress and strain analysis considering a non-uniform thickness profile of REBCO tapes," *IEEE Trans. Appl. Supercond.*, *[Submitted for Publication, 2025]*.

[17] P. Xu, D. K. Bond, I. R. Dixon, and H. Bai, "Stress analysis of terminals from the distribution of screening currents for the 40 T all-superconducting magnet project," *IEEE Trans. Appl. Supercond.*, vol. 33, no. 5, Aug. 2023, Art. no. 4300205, doi: 10.1109/TASC.2023.3253460.